Removal of methyl violet 2B dye from aqueous solution using a magnetic composite as an adsorbent

L.R. Bonetto, F Ferrarini, C. De Marco, J.S. Crespo, Régis Guégan, M Giovanela

▶ To cite this version:

HAL Id: insu-01130235

https://hal-insu.archives-ouvertes.fr/insu-01130235

Submitted on 11 Mar 2015

Removal of methyl violet 2B dye from aqueous solution using a magnetic composite as an adsorbent

L. R. Bonetto[a*], F. Ferrarini[a], C. D. Marco[a], J. S. Crespo[a], R. Guégan[b], M. Giovanela[a*]

[a]Centro de Ciências Exatas e da Tecnologia, Universidade de Caxias do Sul, 95070-560

Caxias do Sul – RS, Brazil.

[b]Institut des Sciences de la Terre d'Orléans, UMR 7327, CNRS-Université d'Orléans, 1A Rue

de la Férollerie, 45071 Orléans Cedex 2, France

Authors to whom correspondence should be addressed: M. Giovanela and L. R. Bonetto.

Phone/Fax: + 55 54 3218 2159. E-mail: mgiovan1@ucs.br and lrbonetto@gmail.com

Abstract

Despite the important role of the textile industry in the global economy, its effluents generate deep concern with regard to treatment and disposal. Adsorption is a promising technique for the removal of textile color effluent at relatively lowcost and with satisfactory efficiency. This study aimed to evaluate the adsorption capacity of a halloysite-magnetite-based compositein the removal of methyl violet 2B cationic dye. Afterpreparation, the obtained composite was characterized by applying several instrumental techniques, includingX-ray diffraction, scanning electron microscopy, energy dispersive spectroscopy and determination of pH at the point of zero charge. The influences ofstirring rate, adsorbent mass, pH,initial concentration ofdyeand contact time on the adsorption process werealso studied. The adsorption capacityof the composite was then investigated in a temperature-controlled batch system. The experimental results showed that the adsorption kinetics were better described using a pseudo-second-order model. Regarding the adsorption equilibrium, the experimental results suggest that both the Langmuir and Freundlich models were applicable. The thermodynamic data showed that dye adsorption onto the composite was spontaneous and endothermic and occurred byphysisorption.The employed composite could also be regeneratedat least four times using a 1.0 mol L^{-1}solution of NaOH as an eluent and was shown to be a promisingadsorbentfor the removal ofcationic dyes.

1 Introduction

Thefuture of Earthandits biodiversityisa common concern foreveryone.Rapid technologicaland industrial developmentin recent decadeshas led to anumber of environmentalproblems, particularly with regardto the pollutionof water resources[1].Synthetic dyes areone of themajor classes ofpollutants responsiblefor imbalancesin aquatic ecosystems; their complexmolecularstructureskeeps themrelatively stable, making them difficultto remove[2].

Color is usually the first contaminant to be recognized in wastewater because a very small amount of synthetic dye in water (< 1.0 mg L^{-1}) is typically highly visible, affecting the aesthetic merit, transparency and gas solubility of water bodies. These dyes absorb and reflect sunlight, thereby interfering with the growth of aquatic species and hindering photosynthesis. Additionally, they can have acute and/or chronic effects on organisms, depending on their concentration and exposure time[3].

Methyl violet (MV) is particularly important because of its broad applications in textiles, paints and print inks[4, 5].MV isoften usedin the dyeingofcotton, silk, paper, bamboo, strawand leather[6]. In biomedical fields, MV is the active ingredient in Gram's biological stain for bacteria classification[7-10]. It can sometimes also be used as a moderate-class disinfectant but has beenfound to be poisonous to most animals. The inhalation of MV may cause irritation to the respiratory tract, whereas ingestion typically causes irritation to the gastrointestinal tract[11].

Dyes can be classified according to their chemical structure or method of application. MV belongs to a class of intensely colored organic compounds called triphenylmethane dyes due to the presenceofthreearylgroups, each of which is bonded toa nitrogen atomthat

interactswith one or twomethyl groups.Moreover, MV is a basic dyebecause of thepresence ofa positive chargeonthe aminogroup[12].

MVis a mixture of tetramethyl, pentamethyl and hexamethyl pararosaniline chlorides[13]. This last chemical compound is also known as *crystal violet* or MV 10B and is the primary representativeof these three dyesreportedin the literature[14-19]. Conversely, in MV 2B,there is a predominance of the pentamethylated compound[13]. Due to this difference, the particular shade of MV differs, depending on the amount of each component present.

Fig. 1showsthe chemical structuresof MV 2B and 10B. The small structural difference observed(the presence of an additionalmethyl group in MV 10B) is responsible for thedifferent physical and chemicalproperties of the two dyes, which include theabsorption maximumin the visible region, solubility, staining intensityandmelting temperature[13].
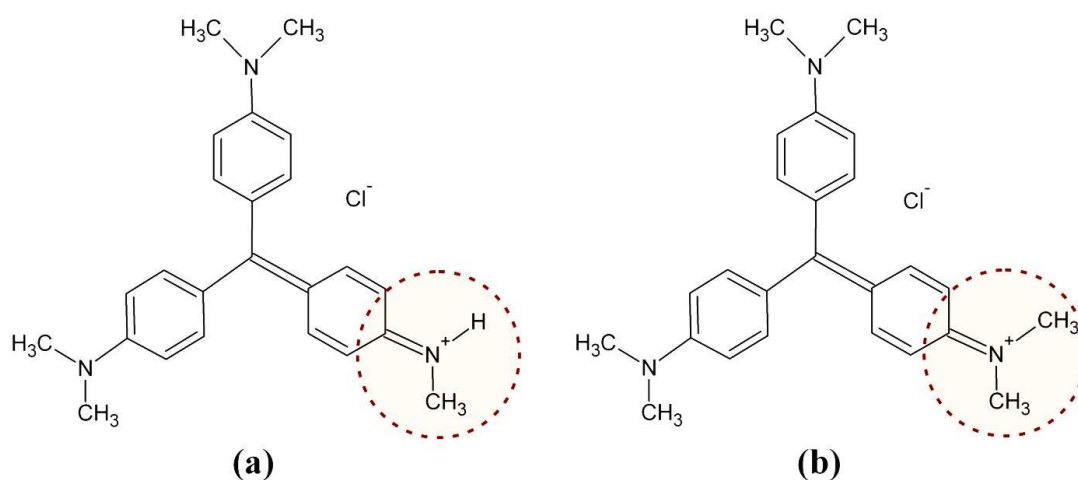

Fig. 1. Chemical structures of MV **(a)**2B and **(b)**10B.

A wide range of technologies has been developed for the removal of synthetic dyes from waters and wastewaters to decrease their environmental impacts. These include physical methods, such as membrane filtration processes and sorption techniques;chemical methods,

such as coagulation, electroflotation, advanced oxidation processes and irradiation; and biological methods, such as aerobic and anaerobic microbial degradation and the use of enzymes[3]. Although chemical and biological methods are effective at removing dyes, they require specialized equipment and are usually energy intensive; in addition, large amounts of by-products are often generated. Conversely, the physical methodsare generally effective at removing dyes without producing unwanted by-products [20, 21].

With regard to the physical methods, sorption of synthetic dyes on inexpensive and efficient solid supports has been considered a simple and economical process for the removal of dyes from water and wastewater, producing high quality water; this process is an attractive alternative for the treatment of contaminated waters, particularly where the sorbent is inexpensive and does not require a pre-treatment step before its application. Sorption is superior to other techniques for water reuse in terms of initial cost, flexibility and simplicity of design, and ease of operation [3].

Activated carbon is the most widely used sorbent, and it has excellent sorption properties for a considerable number of synthetic dyes. However, the preparation of carbon sorbents is generally energy intensive, making commercially available products relatively expensive. Because a large amount of carbon sorbent is needed to remove the dye from a large volume of effluent, high cost can hinder its application [22]. In addition, the technology for manufacturing good-quality activated carbon is not fully availablein developing countries. This limitation has prompted increasing research interest in the production of low-cost alternatives to activated carbon from a range of carbonaceous and mineral precursors[3].

According to Bujdák[23], future investigations could be directed towards the optimization of wastewater treatment processes using suitable clay templatesand nanomaterials. In this way, adsorbents with magnetic properties have been extensively studied by many researchers. Zhao et al. [24] have reported, for example,a novel magnetic

hydroxamic acid modified polyacrylamide/Fe$_3$O$_4$ adsorbent (M-PAM-HA) for the removal of Cd(II), Pb(II), Co(II) and Ni(II) ions from aqueous solutions. Ai et al. [25] and Sun et al. [26] have developeda xylan/poly(acrylic acid) magnetic nanocomposite hydrogel adsorbent and montmorillonite/CoFe$_2$O$_4$ magnetic composite, respectively, for removalof methylene blue from wastewater.

The novelty brought by these adsorbentsis theimprovement in accelerating separation speed, thereby enhancing water treatment efficiency. As a result, solid phase can be easily recovered by the application of an external magnetic field[27-29]. Moreover, adsorbents with magnetic properties produce no contaminants during wastewater treatment. As main disadvantage, most commercially magnetic particles are expensive and cannot be applied to large-scale processes, but magnetic modification of low cost adsorbents could lead to materials suitable for biotechnology and environmental applications[29]. Research hasshown that it ispossible to producepromisingadsorbentsin this field, creating new options for textile industry effluent mitigation[30-36].

Therefore, the aim of this work was to prepare, characterize and evaluate the removal of MV 2B from aqueous solution using a halloysite-magnetite-based composite (HNT–Fe$_3$O$_4$) as an adsorbent. The adsorption kinetics, equilibrium and thermodynamics of MV 2B onto this composite were also investigated.

2 Experimental

2.1 Materials and cleaning procedure

MV 2B (C$_{24}$H$_{28}$N$_3$Cl, Color Index 42535) was purchased from VetecQuímica Fina Ltda (Rio de Janeiro, RJ, Brazil). HNT and iron salts (FeCl$_3$. 6 H$_2$O and FeSO$_4$. 7 H$_2$O) were

acquired from Sigma-Aldrich (São Paulo, Brazil). The chemicals used in this work were of analyticalquality and were used without further purification. All aqueous solutions, including solutions of KNO_3, KOH, HNO_3, HCl and $NaOH$ (Merck, São Paulo, SP, Brazil),were prepared using deionized water (18.2 MΩ cm resistivity) obtained from a Millipore Milli-Q UV Direct-Q 3 UV system (Darmstadt, Germany).

All laboratory glassware used in the preparation of the HNT-Fe_3O_4 composite and in the adsorption experimentswas first washed with tap water and then soaked in an alkaline Extran solution (15% v/v) for 24 h. After this period, they were washed thoroughly with tap water and then soaked in a solution of HNO_3 (5% v/v) for 24 h. Finally, the material was rinsed with deionized water and left to dry at room temperature.

2.2 Preparation of HNT-Fe_3O_4 composite

The HNT-Fe_3O_4 composite was prepared using the chemical precipitation method [31]. Initially, 6.25 g of HNT was added into a 500 mL solution of 7.275 g of $FeCl_3$. 6 H_2O and 3.75 g of $FeSO_4$. 7 H_2O. The suspension was thenrefluxed for 3hin aglycerin bathat 120°C undernitrogen gas flow. When the mixed suspension was cooledto 50°C, NaOH solution (4.0 molL^{-1}) was addeddropwise with vigorousmagnetic stirring. ThepH of the final suspension was controlled to be in the range of 9.0–10.0. The mixture was aged at 50°C for 2.5 h and then filtered and washed with deionized water repeatedly. At the end of this procedure, the obtained composite was dried at 60°C for 24 h.

2.3 Characterization of HNT-Fe_3O_4 composite

The crystalline phases in the HNT and HNT-Fe$_3$O$_4$ composite were characterized by X-ray powder diffraction using a Shimadzu XRD-6000 diffractometer (Tokyo, Japan). The samples were scanned at room temperature in reflection mode using incident CuK$_\alpha$ radiation ($\lambda = 1.5405$ Å) at a step width of 0.05° min^{-1} from $2\theta = 2°$ to 80°.

The morphology of the HNT and HNT-Fe$_3$O$_4$ composite was examined by scanning electron microscopy (SEM) using a ShimadzuSSX-550 (Tokyo, Japan) operating at an accelerating voltage of 10 kV. Before analysis, the samples were sputter-coated with a thin gold layer for 2.5 min. The qualitative analysis of iron in the HNT-Fe$_3$O$_4$ compositewas performed by energy dispersive spectroscopy (EDS) of the same sample used in the SEM analysis and in the same microscope, operating at an accelerating voltage of 15 kV.

Nitrogen adsorption-desorption experiments were performed in order to obtain information on the specific surface area of the HNT-Fe$_3$O$_4$ composite. The measurements were carried out at 77 K using a Quantachrome Instruments Nova 2200e Surface Area Analyzer (Boynton Beach, FL, United States of America). About 100 mg of the sample was outgassed at 383 K for 24 h under a residual pressure of 0.01 Pa. Data were recorded for relative vapour pressures from 0.05 to 0.99. The specific surface area was determined using the Brunauer-Emmet-Teller (BET) equation based upon the cross-sectional area of nitrogen (0.163 nm^2) at 77 K.

The point of zero charge (pH$_{PZC}$) of the HNT-Fe$_3$O$_4$ composite was determined by adding 50 mL of 0.01 mol L^{-1} KNO$_3$ with a previously adjusted initial pH (i.e., pH$_i$ values of the solutions were adjusted from 2.0 to 11.0 with 0.10 mol L^{-1} of KOH or HNO$_3$) to several 150 mL Erlenmeyer flasks. Each Erlenmeyer contained 0.10 g of the magnetic compositeand was securely capped immediately with a sheet of aluminum foil. Then,the Erlenmeyers were shaken at a stirring rate of 400 rpm using a thermostated water bath shakerat a constant temperature of 25°C; the samples were then allowed to equilibrate for 24 h. At the end of this

experimental procedure, the suspensions were filtered, and the final pH (pH_f) values of the solutions were recorded using a Digimed DM-20 pHmeter (São Paulo, SP, Brazil). The value of pH_{PZC} is the point where the curve of ΔpH ($pH_i - pH_f$) versus pH_i crosses the line equal to zero[37].

2.4 Adsorption experiments

The adsorption experiments were performed in a Dist multiple spindle stirrer (Florianópolis, SC, Brazil) using 25 mL of dye solution at 25°C for 6 h. Subsequently, the Erlenmeyers were exposed to a magnetic field using a 3000 G magnet for 5 min to separate the magnetic composite from the aqueous solutions.

The initial and final concentrations of the MV 2B remaining in the solutions were determined by visible spectrophotometry using a Thermo Scientific Evolution 60 spectrophotometer (Waltham, MA, United States of America) fitted with a quartz cellwith a path length of1.0 cm. Absorbance measurements were made at 582 nm (i.e., the maximum wavelength of MV 2B dye). A calibration curve was constructed withdye concentrations ranging from 1.0 to 15.0 mg L^{-1}.

The removal percentage (*%R*, %), the amount of MV 2B adsorbed at time *t* (q_t, mg g^{-1}), and the adsorption capacity at equilibrium (q_e, mg g^{-1}) were calculated by applying Equations (1), (2) and(3), respectively[31, 33]:

$$\%R = \frac{(C_0 - C_t)}{C_0} \times 100 \tag{1}$$

$$q_t = \frac{(C_0 - C_t)}{m} \times V \tag{2}$$

9

$$q_e = \frac{(C_0 - C_e)}{m} \times V \quad (3)$$

where C_0, C_t and C_e are the concentrations of MV 2B initially, at time t and at equilibrium, respectively (mg L^{-1}); m is the weight of the HNT-Fe$_3$O$_4$ composite (g); and V is the volume of the MV 2B solution (L).

3 Results and discussion

3.1 Preparation and characterization of HNT-Fe$_3$O$_4$ composite

3.1.1 X-ray diffraction (XRD)

The XRD patterns of the HNT and HNT-Fe$_3$O$_4$ composite are shown in **Fig. 2**. The new diffraction peaks at 35.45° (3 1 1), 43.20° (4 0 0), 57.15° (5 1 1) and 62.75° (4 4 0) can be identified as Fe$_3$O$_4$, while the other diffraction peaks at 12.29° (0 0 1), 19.78° (0 2 0) and 24.99° (0 0 2) can be indexed to HNT[31, 33, 38]. These results indicated that magnetic particles were successfully anchored onto the surface of the clay.
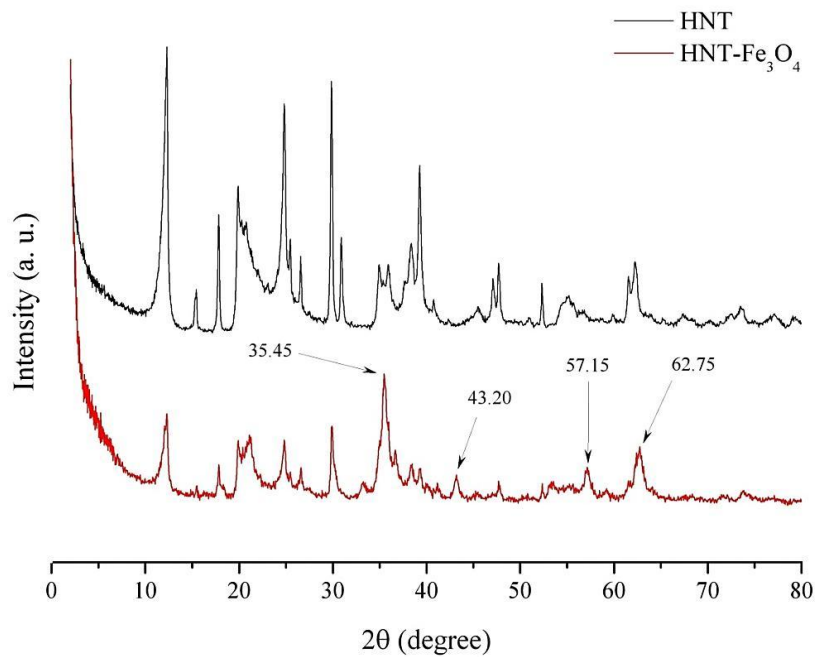
Fig. 2. XRD patterns of the HNT and HNT-Fe$_3$O$_4$ composite.

3.1.2Scanning electron microscopy (SEM) and energy dispersive spectrometry (EDS)

Fig. 3shows the SEM images and EDS spectra for the HNT andthe HNT-Fe$_3$O$_4$ composite.As shown in the **Fig. 3(a)**, HNT nanotubes are of different sizes with open ends. Conversely, the SEM image of the HNT–Fe$_3$O$_4$ composite (**Fig. 3(b)**)shows that theFe$_3$O$_4$nanoparticlesareadheredto the surfaceof theHNT nanotubes;this is corroborated by the XRD analysis.

EDSspectrafor both materials(**Figs. 3(c)**and**3(d)**) confirmed the presenceofaluminum, oxygen and siliconelements, whichare characteristic ofaluminosilicates, as well as ironin thecompositedue toits coveringof Fe$_3$O$_4$nanoparticles. Inboth samples, goldwasalsodetecteddue to thethinlayer depositedtoperform these analyses.
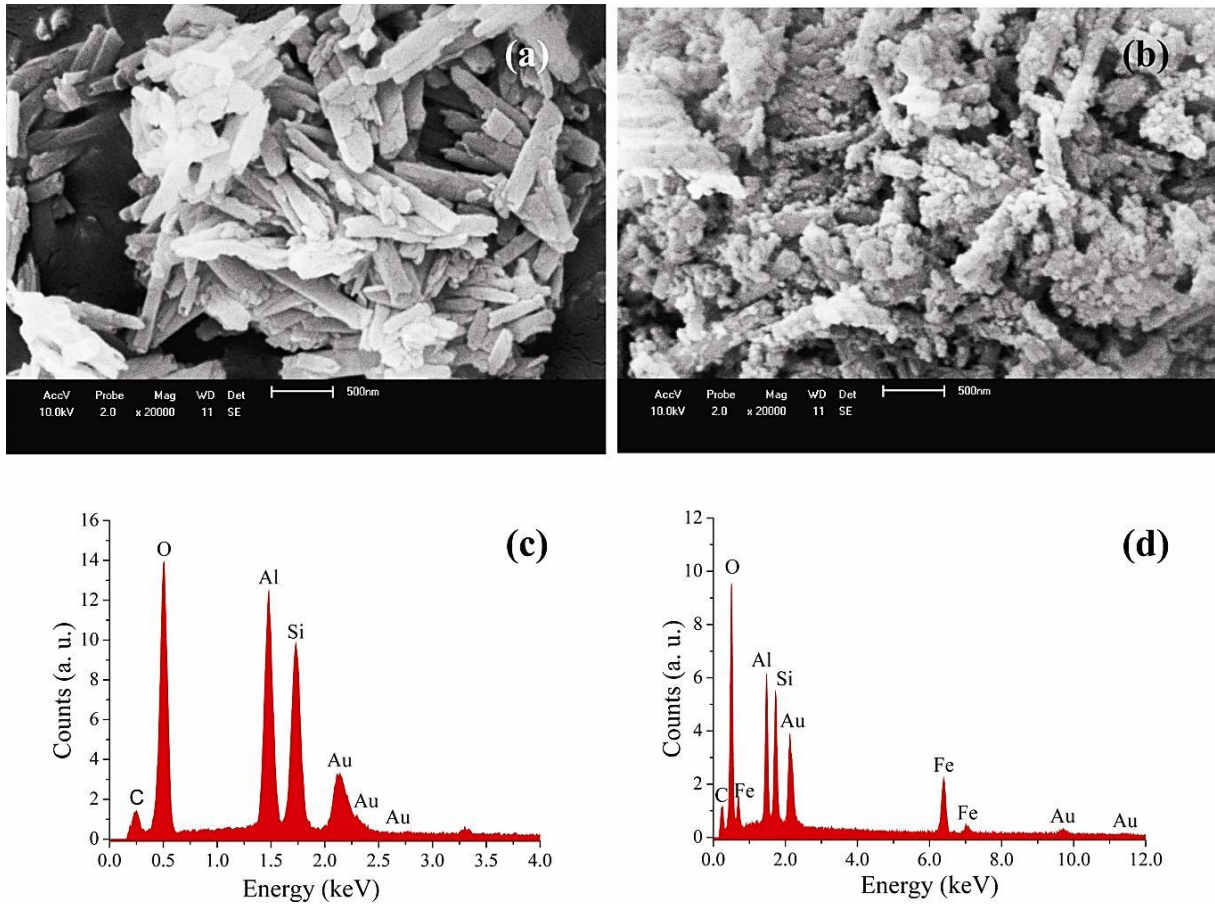
Fig. 3.(a) SEM image of HNT; **(b)** SEM image of HNT-Fe$_3$O$_4$ composite; **(c)**EDS spectrum of HNT; and**(d)** EDS spectrum of HNT-Fe$_3$O$_4$ composite.

3.1.3 BET analysis

The adsorption and desorption isotherms of nitrogen gas revealed classical features for both non swelling clay mineral and iron oxides. The BET calculation applied to the nitrogen desorption isotherm gave a total specific surface area for the HNT-Fe$_3$O$_4$ composite of 46 m^2 g^{-1}, an intermediate value between the starting materials for which their specific surface area was reported to be in the range of 50-60 and almost 9m^2 g^{-1}for kaolinite-halloysite clay minerals [39]and magnetite particles[40], respectively.

12

3.1.4pH$_{PZC}$ determination

The pH$_{PZC}$curve of the HNT-Fe$_3$O$_4$ composite is shown in **Fig. 4**. The pH$_{PZC}$ is the pH value where positive and negative charges are equal on the surface of a material, which makes it possible to describe the properties of the resulting electrical double layer interfaces [41].

For pH values lower than pH$_{PZC}$, the adsorbent presents a positive surface charge that favors the adsorption of negatively charged compounds, such as anionic dyes. In the situation when the pH is greater than pH$_{PZC}$, the adsorbent presents a negative surface charge that favors the adsorption of positively charged compounds, such as MV 2B [37]. Thus, it can be concluded that the adsorption of this dye by HNT-Fe$_3$O$_4$ composite should be favored in media with a pH greater than 5.02.
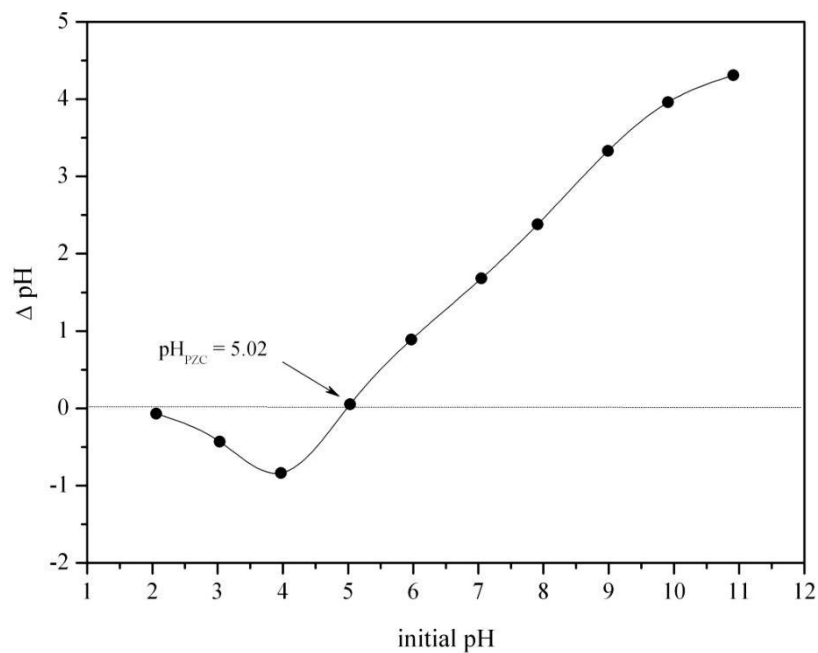
Fig. 4. Curve of the point of zero charge (pH$_{PZC}$) of the HNT-Fe$_3$O$_4$ composite.

Note: the horizontal dotted line shown is used only as a visual guide.

3.2 Effect of experimental conditions on the adsorption process

To evaluatethe effect of the experimental conditions on theadsorptionprocess(e.g., stirring rate,adsorbent dosage, initial pH, initial dye concentrationand contact time), the results were comparedin termsof *%R* and q_t, which were calculatedusing Equations(1)and (2), respectively. For this calculation, it wasnecessary to know thevalue of the finaldye concentrationat the endof each experiment as obtainedusing acalibration curve(r=0.9997).

3.2.1 Stirring rate

The experiments used to evaluatethe influence of thestirring rateonthe adsorption processwere conductedin aDist multiplestirrerspindle at 25°Cwithan initialweightof 0.15 gof compositein 25mL of 90 mgL^{-1} of MV2B(pH~4.2)for 6 h.The effect of the stirring rate on the dye removal percentage is shown in **Fig. 5**.
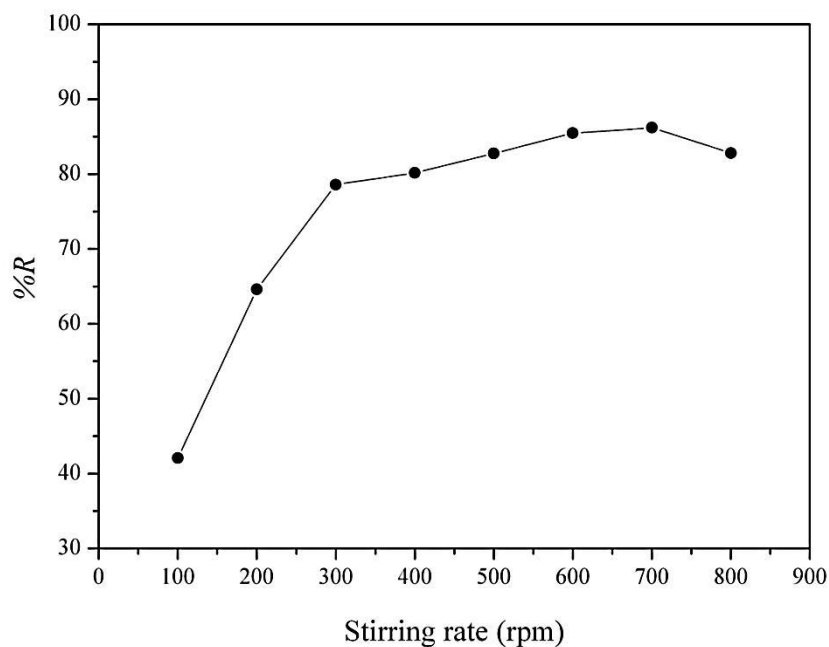

Fig. 5. Effect of the stirring rate on the MV 2B removal percentage.

As shown, *%R* increases as the stirring rate of the system increases, indicating the occurrence of a stronger interaction between the composite and the dye. Furthermore, a higher removal percentage occurs when the stirring rate of the system is equal to 700 rpm. For higher values, the *%R* begins to decrease; the associated high rate of turbulence in this case might promote the entrainment of the MV 2B particles before they can interact with the composite. The decrease in percentage removal may also be explained by the fluid dragging $HNT-Fe_3O_4$ particles due to the high rate of the system, which also affects the interaction of the composite with the dye[42].

3.2.2 Adsorbent dosage

The experiments performedto evaluatethe influence of theadsorbent massonthe adsorption processwere also conductedin aDist multiplestirrerspindle at 25°C with0.025, 0.05, 0.10, 0.15, 0.20 and 0.25 g of composite. A volume of25mL ofMV2Bat a concentration of90 mgL^{-1} was used,with the stirring rate previously optimizedat apH value of approximately4.2for 6 h.The adsorbent dosage effect on the MV 2B removal percentage is shown in **Fig. 6**.
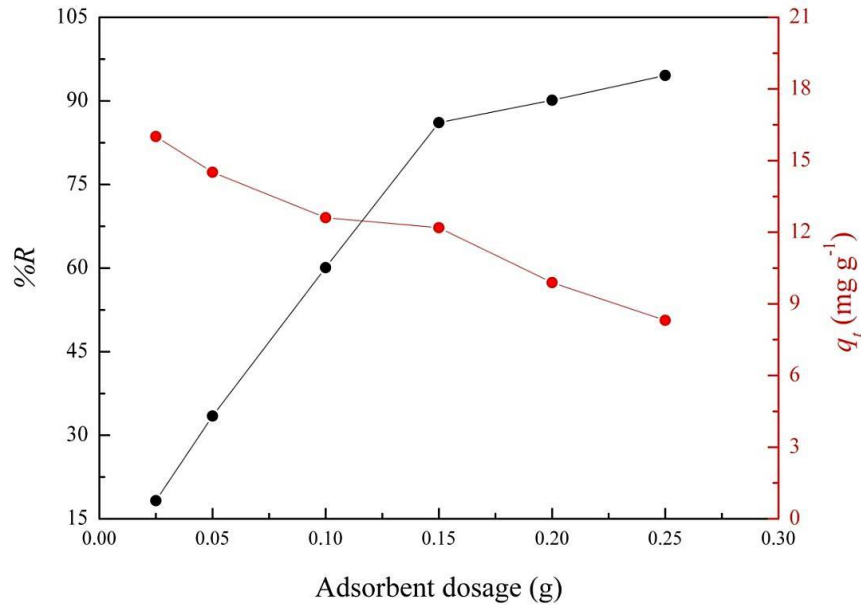
Fig. 6. Effect of the adsorbent dosage on the MV 2B removal percentage.

The results show that *%R* increases as the adsorbent dosage increases. It was found that the MV 2B removal percentage increased from 18.3% to 94.7% when the adsorbent dosage was increased from 0.025 to 0.25 g. This increase likely occurreddue the increment of the number of adsorption sites available for adsorption [43]. However, $q_t$shows the opposite behavior of the removal percentage, likely due to the increase in the adsorbent mass at a determined dye concentration;fixed volume also leads to unsaturated adsorption sites during the adsorption process. Additionally,a high adsorbent mass may be favorable to particle aggregation, which would lead a decrease in total surface area of the adsorbent and an increase in diffusional path length[43].In addition, this reduction of q_t can be mathematically explained by combining Equations (1) and (2), as shown in Equation (4):

$$q_t = \frac{\%RC_0V}{100\,m} \tag{4}$$

16

where *%R* is the removal percentage (%), C_0 is initial concentration of MV 2B (mg L^{-1}), *m* is the weight of HNT-Fe$_3$O$_4$ composite (g), *V* is the volume of MV 2B solution (L), and $q_t$is the amount of MV 2B adsorbed at time *t* (mg g^{-1}).

According toEquation (4), the amount of dye adsorbed at a time *t* (q_t) and the mass of adsorbent (*m*) are inversely proportional. For fixed values of the dye percentage removal (*%R*), the treated volume of dye solution (*V*) and the initial dye concentration (C_0), the increase of adsorbent mass leads to a decrease in $q_t$values [44].

Based on these results, the value of adsorbent mass should be chosen based on the intersection of the curves *%R* and q_t with the justification that this location will produce the most cost-effective system [31]. However, for the adsorption experiments, an adsorbent amount of 0.15 gwas chosen because this dosage results in a satisfactory removal percentage (i.e., above 85%) and q_t values (e.g., 12.18 mg g^{-1}), particularly when compared to 0.10 g, which typically yields a removal percentage ofapproximately 60% and a $q_t$of 12.61 mg g^{-1}. The use of an amount greater than 0.15 g does not show significant advantages in terms of percent removal with an increase of approximately 5%.

3.2.3 Initial pH

To optimize pH, experiments were performed with a range of values between 3.0 and 11.0 in increments of unity, adjusted by adding HCl or NaOH solutions. The concentration of the MV 2B solution was set to 90 mg L^{-1} by applying the stirring rate and adsorbent dosage previously determined to be optimal (i.e., 700 rpm and 0.15 g, respectively)for 6 h at 25°C.The effect of the initial pH on the MV 2B removal percentage is shown in **Fig. 7**.
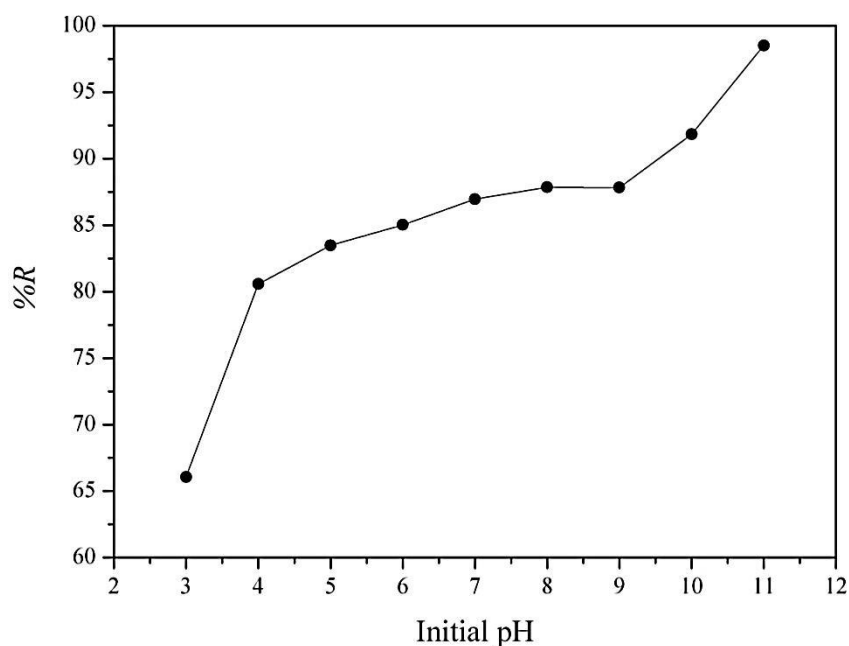
Fig. 7. Effect of initial pH on the MV 2B removal percentage.

As shown, *%R* increases as pH increases. In an acidic medium, little interaction occurs between the adsorbent and adsorbate. This behavior is expected because the pH_{PZC} value of the adsorbent is lower than 7.0. Under these conditions, the $HNT-Fe_3O_4$ composite is positively charged (i.e., with the same net charge as the dye), resulting in electrostatic repulsion between the composite and the dye. For pH values lower than 3.2, MV 2B begins to change color towards yellow, which ultimately changes the maximum absorption in the visible region. All of these factors result in a non-optimal scenario for adsorption.

In systems with higher pH(e.g., 9.0 to 11.0), there is a large increasein *%R*,includingvalues near100% at pH11.0. According toDuynsteeandGrunwald[45], in the pH rangebetween9.0and 13.0,a reactionbetweenthe dyeandOH^-ions occurs. These ions attack the central carbon atom of the MV 2B molecule, forming a base carbinol with a different molecular geometry.Theresulting compoundhas nocolor,which explainsthe high *%R*values in thispH range.

Despite thenearly complete removal ofcolor, as shownby the high*%R* value,the dye still remains in solution. Whenthesecarbinolbases form, the absorption peakshifts tothe UVregion, making it difficult to study theadsorption processofthecomposite because the calibration curveused to quantifythe dyewas constructedusing themaximum absorptionof the dyeat582nm. Finally, theOH⁻ionscompetewith the adsorbent in the interactionwithMV2B molecules.

Based on these observations, the best conditionsfor adsorption are in the range ofpH valuesbetween 5.0and 9.0; this is the range whereremoval is improvedwithout a loss of colordue tochemical reactions. Because of the differencesin percentageremovalvarybyonly 5%, aneutral pH value was adopted for this study.Furthermore, at this pH value(which is higher than the pH_{PZC} of the $HNT-Fe_3O_4$ composite) the adsorbent surface is now completely negatively charged and, as a result, itcan better interact with the MV 2B molecules (positively charged) by electrostatic interactions favoring the adsorption process (**Fig. 8**).
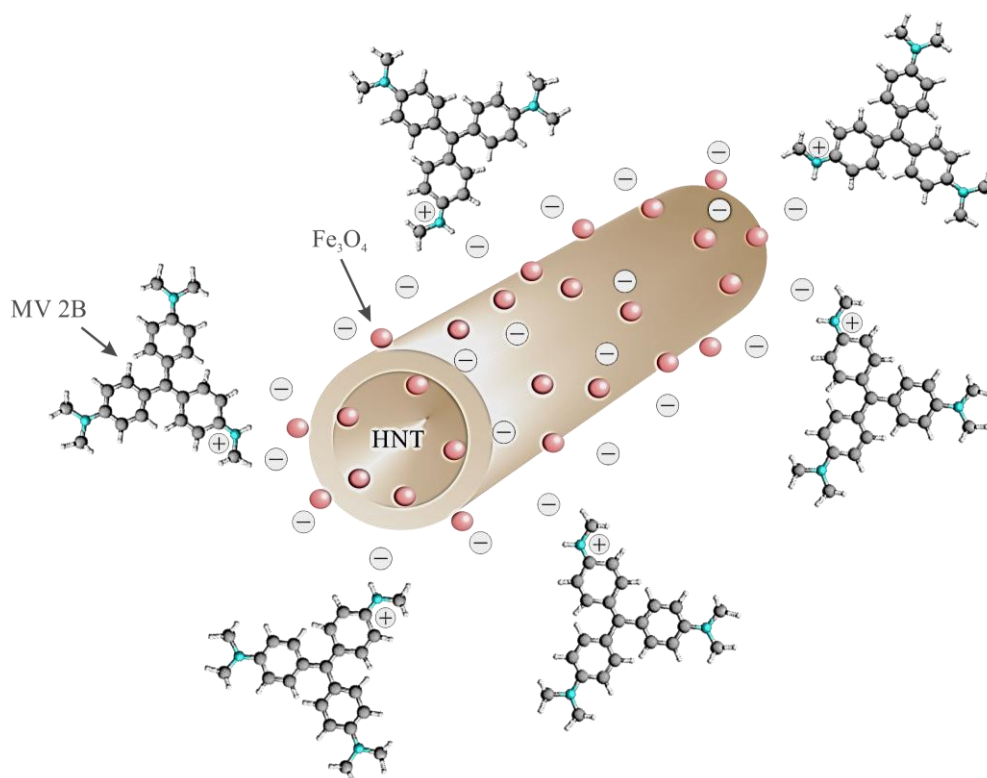
Fig. 8. Electrostatic interactions between MV 2B molecules and HNT-Fe$_3$O$_4$ composite at pH values higher than the pH$_{PZC}$ of the adsorbent.

3.2.4 Effect of initial dye concentration and contact time

To optimizethe initial concentration of dye and contact time on the adsorption process, experiments wereconductedwith 25 mLofMV2Bat concentrations of60, 90,120, 150 and180 mgL^{-1}over time intervalsof 10, 20, 40, 60, 90, 120, 150, 180, 240 and360min. The stirring rate, adsorbent dosage and initial pH used were those previously optimized at 25°C.

As shown in **Fig. 9**, $q_t$increases as the initial concentration of MV 2B in solution increases; however, these values tend to be constant after a certain period of time. The increase in $q_t$in the experiments that contained higher initial concentrations of dye can be explained by the existence of a higher concentration gradient of MV 2B, which increases the diffusive contribution of the mass transfer process[31, 46].This increasein the values of$q_t$at equilibriumdoes not follow aproportionality,presentingshorter intervalsas theinitial concentrationof MV2Bincreases, particularlyat higherconcentrations. According toGusmãoet al.[47], this is an indicationthat theremoval percentagedecreases asthe initial concentrationof MV2Bincreasesdue to the greateramount ofdye presentin the bulk solution. The mass of HNT-Fe$_3$O$_4$composite used (i.e., 0.15 g)islikely not sufficient to promotea high-percentageremovalforhigher concentrations, as discussed in section 3.2.2; this is alsoin accordance withHameed[48].Theadsorbeddye moleculeslikely exert anelectrostatic repulsiononthose stillin solution, increasing resistance to mass transfer.
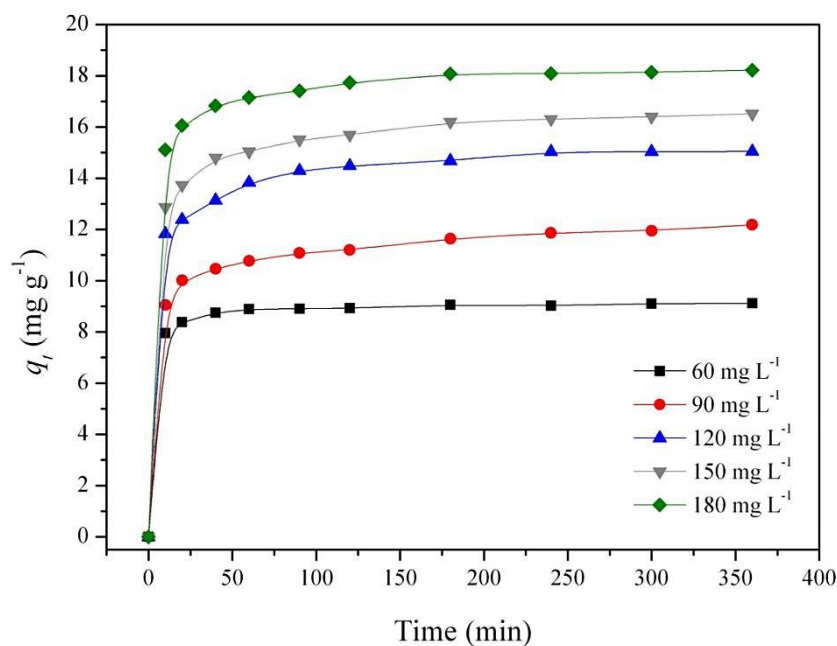
Fig. 9. Effect of the initial dye concentration and contact time on the adsorption process.

Regarding the influenceof thecontact time,$q_t$is shown to increase as theprocess evolvesuntil equilibriumis reacheddueto the longer period,so thatthe interaction betweenthe soluteandcompositeoccurs, increasing the amount ofadsorbedMV2B [31].However, thecurves shown in**Fig. 9** show thatthe removal isfasterin the initial minutesofthe processbecausemore adsorption sites are available during this period. Asthese sites become progressivelyoccupied, adsorptionbecomesslowerand less efficient[37]. Another important aspectto note isthat as the initial concentration ofMV2B increases, moretime is required forequilibrium to be reached. The reasonfor this phenomenon is thata higher concentration ofadsorbatein the solutionincreases theelectrostatic repulsionbetween moleculespresent in the medium, increasing the diffusive resistancetomass transferwithinthesolution but notin the interfaceas previouslydiscussed; this results in a slower process[48].

3.3 Adsorption kinetics

To identifythe mechanism ofadsorption, the potentialremoval rateand the controlof the steps involvedin the process,two kineticmodels(i.e., thepseudo-first- and pseudo-second-order)can be adopted [46]. Kinetics experiments were performed at the same conditions as described in the section 3.2.4. The pseudo-first- and pseudo-second-order kinetic models are shown in **Fig.10**.
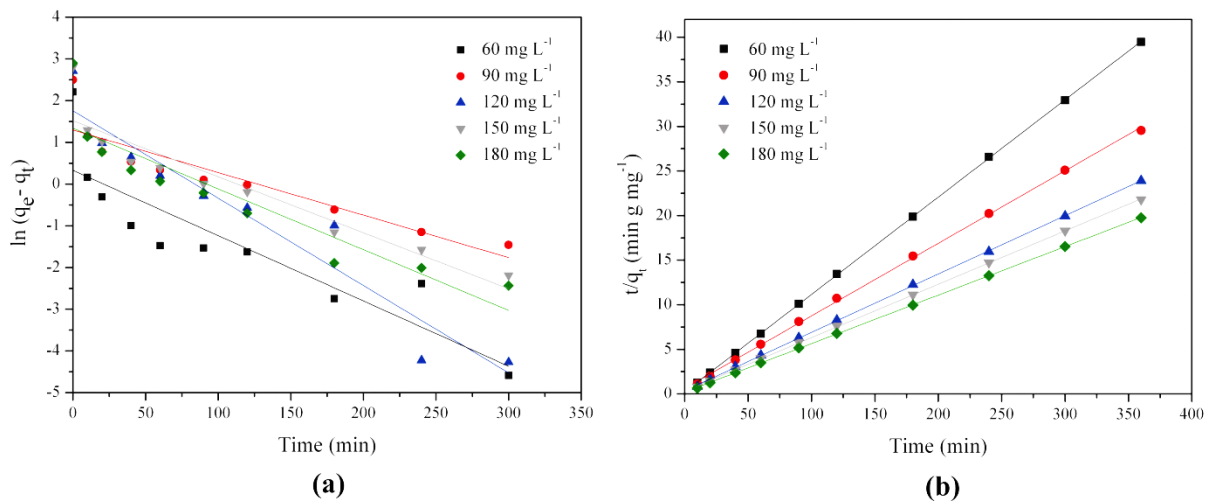

Fig. 10. Kinetics experimental results: **(a)** pseudo-first- and **(b)** pseudo-second-order.

Thepseudo-first order kinetic modelcanbe expressedbyEquation(5)[49]:

$$\ln(q_e - q_t) = \ln q_e - k_1 t \quad (5)$$

where k_1 is the pseudo-first-order rate constant (min^{-1}). The k_1 and q_e parameters can be determined from the slopeandintersection of the linesoflog (q_e-q_t) versus t. These values are summarized in Table 1.

The coefficientof correlation (r) for thepseudo-first-ordermodelrangedfrom 0.8734 to 0.9566forinitial concentrationsof MV2Bof60, 90, 120, 150 and 180 mg L^{-1}.The experimental valuesof q_e,(q_{eexp}, mg g^{-1}) diverged fromthe calculated values($q_{e\ cal}$, mg g^{-1}), as shownin Table 1. This result indicates thatthe adsorption ofthe MV 2B by the compositedoes not follow thepseudo-first-orderkinetic model(i.e., the process is nota phenomenon controlled bydiffusion;othersteps areresponsible for controlling thekinetics observed).Therate constant$k_1$can be interpretedas atemporalscalefactor, which is intended toindicate therate at whichthe systemreaches equilibrium.Higher values of$k_1$indicate lesstime to reachthat condition and vice versa. This parametermay or may notbe dependent onthe experimental conditionsof the process[49].As shown in Table1, the adsorption process does not reachequilibriumin a short periodaccording to the pseudo-first-order model becausethe values of$k_1$are on the orderof10^{-2},withthe greatest differenceoccurringin the experimentsin which the initialdye concentrationsare 90 and 120mg L^{-1}.This findingalso indicates that k_1 does not depend on the initial concentration of MV 2B parameter.

The pseudo-second-order kinetic model can be expressed by Equation (6)[50]:

$$\frac{t}{q_t} = \frac{1}{k_2 q_e{}^{\mathbf{2}}} + \frac{1}{q_e}t (6)$$

where k_2 is the pseudo-second-order rate constant (g mg^{-1} min^{-1}). Analogous to thepseudo-first-orderkinetic model, the $k_2$and$q_e$parameters weredetermined from thelinearand angularcoefficients of the equationsformedby regressing$t$/$q_t$versus t, respectively. The$r$valueat

different concentrationsof the linearportionsis greater than0.9997, which suggests that the adsorptionoftheMV 2Bfollows thepseudo-second-orderkinetic modelwherein therateof chemicalinteractions between thedye andthe sites ofadsorbent isthe step thatcontrols theoverallkinetics of the process. Furthermore, the calculated data ($q_{e,cal}$) are consistent with the experimental data ($q_{e,exp}$), as shown in Table 1.

Table 1

Kinetics parameters for MV 2B adsorption by HNT-Fe$_3$O$_4$ composite.

	Initial dye concentration (mg L^{-1})				
	60	90	120	150	180
$q_{e,\,exp}$ **(mg g^{-1})**	**9.12**	**12.18**	**15.05**	**16.72**	**18.23**
Pseudo-first-order					
$q_{e,\,cal}$ (mg g^{-1})	1.39	3.65	5.79	4.56	3.81
$k_1 \times 10^2$ (min^{-1})	1.57	1.02	2.09	1.34	1.46
r	0.8734	0.9021	0.9566	0.9315	0.9079
Pseudo-second-order					
$q_{e,\,cal}$ (mg g^{-1})	9.16	12.29	15.29	16.69	18.37
$k_2 \times 10^2$ (g mg^{-1} min^{-1})	5.24	1.11	1.24	1.10	1.55
r	0.9999	0.9997	0.9999	0.9999	0.9999

Thekinetic constantk_2 has the same physicalmeaningas $k_1$and mayor may not alsodepend onthe experimental conditionsof the adsorption process[49]. In this case, the results shown in Table 1 demonstrate that k_2 does not depend on the initial concentration of MV 2B parameter either. The results of$k_2$are also on theorder of10^{-2}, which indicatesthat adsorptiondid notreachequilibriumwithin a short time period, according to the pseudo-second-

order model.Unlike whatwaspreviouslyobserved, the value of$k_2$differs slightlyin experiments with lowerMV2B concentrations (C_0 = 60 mg L^{-1}) than for the other experiments, which show a valueapproximately 4times higher, indicating thatequilibrium is attained more rapidlyunder these conditions.

3.4 Adsorption equilibrium

Adsorption isotherm modelsare fundamentalto describing the interactive behavior between theadsorbateandadsorbent and are also important for investigating mechanisms of adsorption. In this study, equilibrium data were analyzed using the Freundlich and Langmuir isotherms. It is important to emphasize that the equilibrium experiments were performed at the same conditions of adsorption kinetics.

To evaluate which model was best suited to describe these processes, *r* and the error function(F_{error}) were analyzed; a lower result from the error function indicated a smaller difference between adsorption capacity calculated by the model (q_{cal}) and the experimental (q_{exp}). F_{error}canbe expressedaccording toEquation (7)[51]:

$$F_{error} = \sum_{i}^{P} \left(\frac{q_{i\,cal} - q_{i\,exp}}{q_{i\,exp}} \right)^2 \qquad (7)$$

where $q_{i\,cal}$ is a value of q predicted by the fitted model;$q_{i\,exp}$ is a value of q measured experimentally;*i* indicatesthe values of the initial dye concentration of the experiments (60, 90, 120, 150 and 180 mg L^{-1}); and *P*is the number of experiments performed.

The Freundlich and Langmuir isotherm linearized models are shown in **Fig. 11**.
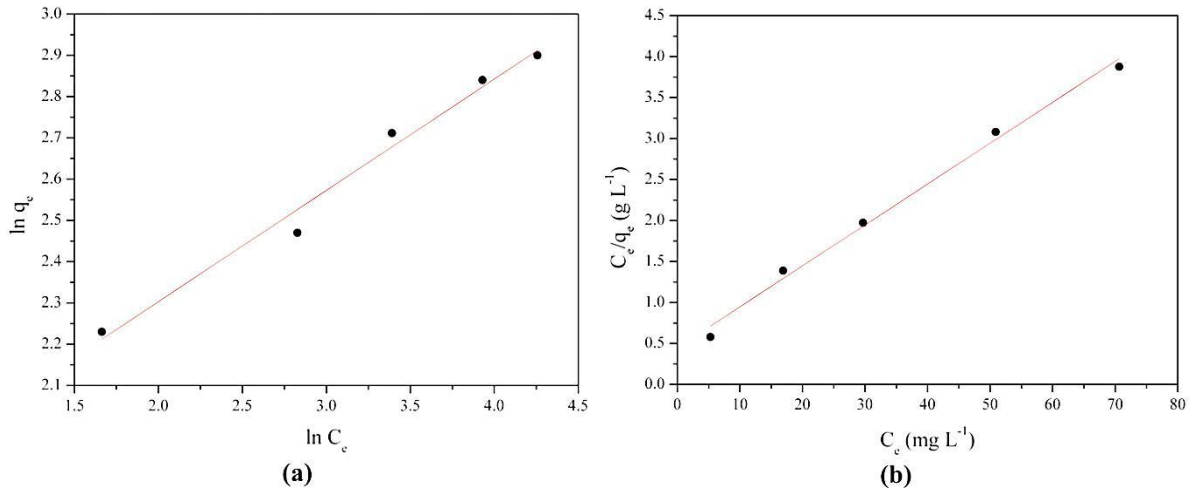
Fig. 11.(a) Freundlich and **(b)** Langmuir isotherm linearized models.

The empirical Freundlich equation is applicable to adsorption on heterogeneous surfaces, where the interaction between the adsorbed molecules is not limited to the formation of a monolayer. The Freundlich constant (k_F) is related to the adsorption capacity of the adsorbent: the higher the value, the greater the affinity for the adsorbate. The empirical parameter $1/n$ is related to the strength of adsorption, which varies with the heterogeneity of the material. When the values of $1/n$ are between 0.1 and 1.0, the adsorption process is considered favorable [46]. The linearized form of the Freundlich equation is expressed according to Equation (8)[52]:

$$\ln q_e = \ln k_F + \frac{1}{n}\ln C_e \ (8)$$

where k_F is the Freundlich constant (L g^{-1}) and $1/n$ is a dimensionless empirical parameter. The k_F and $1/n$ values were determined from the linear and angular coefficients of the equations formed by regressing $\ln q_e$ as a function of $\ln C_e$, respectively. These values, along with r and F_{error}, are shown in Table 2. In general, the experimental data are shown to be well

26

adjusted to the Freundlich model because the *r* value is greater than 0.98, and F_{error} is near 0.0022.The value of 0.2696 for the parameter $1/n$ is lower than 1.0, suggesting that the adsorption is favorable under the conditions proposed by the Freundlich model.

The Langmuir model is based on the assumption of monolayer adsorption on a structurally homogeneous adsorbent, where all sorption sites are identical and energetically equivalent [42]. The linearform of theLangmuirequation canbe expressedaccording toEquation (9)[52]:

$$\frac{C_e}{q_e} = \frac{C_e}{q_m} + \frac{1}{q_m k_L}\,(9)$$

where q_m is the theoretical maximum adsorption capacity corresponding to monolayer coverage (mg g^{-1}), and k_L is the Langmuir constant (L mg^{-1}). The k_L and $q_m$weredetermined from thelinearand angularcoefficients of the equationsformedby regressingC_e/q_e as a function of C_e, respectively.

To determine whether the adsorption process is favorable, a dimensionless constant separation factor R_L is defined. The adsorption process is irreversible when R_L is 0.0, favorable when R_L is between 0.0 and 1.0, linear when R_L is equal to 1.0, and unfavorable when R_L is greater than 1.0. The R_L parameter can be defined based on Equation (10)[52]:

$$R_L = \frac{1}{1 + k_L C_0}\,(10)$$

where C_0 is the initial dye concentration (mg L^{-1}).

The isotherm parameters for MV 2B adsorption by the HNT-Fe$_3$O$_4$ composite are shown in Table 2. As shown, the experimental data are well adjusted to the Langmuir modelas well. The R_L values are between 0.130–0.048, confirming that the adsorption process is also favorable. Although the r value is greater than 0.99, its F_{error} is higher than 0.04 and, thus, higher than the one obtained for the Freundlich model. It can be inferred that analyzing the correlation coefficient of the fitting is not the only parameter that should be account for to verify the best fitting isotherm model. Thus, thesedata suggest that both models were suitably fitted [53]. Similar results were also observed by Lima et al. [51], Namasivayam and Sureshkumar [54], and Kalavathy and Miranda [55]. According to these authors, the adsorption mechanism by both monolayer adsorption and heterogeneous energetic distribution of active sites on the adsorbent surface is possible [54].

Table 2

Isotherm parameters for MV 2B adsorption by HNT-Fe$_3$O$_4$ composite.

Isotherm		Temperature (25°C)
Freundlich	k_F (L g^{-1})	5.835
	$1/n$	0.2696
	r	0.9892
	F_{error}	0.0022
Langmuir	q_m(mg g^{-1})	20.04
	k_L (L mg^{-1})	0.112
	R_L	0.130–0.048
	r	0.9955
	F_{error}	0.0417

A comparison of the q_m of a few adsorbents available in the literature for removal of MV 2B in aqueous solution is given in Table 3.It is clear shown that HNT-Fe_3O_4 composite used in this work had a moderate adsorption capacity, despite of its relatively small surface area.

Table 3

Comparison of maximum adsorption capacity(q_m) of other adsorbents for removal of MV 2B.

Adsorbent	q_m (mg g^{-1})	Reference
Modified cation exchange membrane	10.1	[56]
Cellulose-based wastes	10.5	[57]
Mansonia wood sawdust	16.11	[58]
HNT-Fe_3O_4 composite	20.04	This study
Sunflower seed hull	92.59	[48]

3.5 Thermodynamics studies

Thermodynamics experiments were performed at 283, 293 and 303 K at an initial dye concentration of 90 mg L^{-1}. This initial concentrationwas chosenbecause it provided the best opportunity to monitorthe adsorption process.The other conditions used were the same as those used in the kinetics and equilibrium studies.

The values of the standard Gibbs free energy change ($\Delta G°$) for each temperature were calculated from the Equation(11)[59]:

$$\Delta G^o = -RT \ln k_c \qquad (11)$$

where R is the universal gas constant (8.314 J mol^{-1} K^{-1}),T is temperature (K) andk_c is the equilibrium stability constant, which was calculated at each temperature by the Equation (12)[59]:

$$k_c = \frac{C_s}{C_e} \quad (12)$$

where C_s and C_e are the equilibrium concentrations on the adsorbent and on the aqueous phase, respectively.

The enthalpy change ($\Delta H°$) and entropy change ($\Delta S°$) are calculated from the slope and intercept of the plot of ln $k_c$versus1/T, based on the Van't Hoff equation (Equation 13)[59]:

$$\ln k_c = \left(\frac{\Delta S°}{R}\right) - \left(\frac{\Delta H°}{R}\right)\frac{1}{T} \quad (13)$$

The results of the thermodynamics experiments are shown in Table 4. The negative values of $\Delta G°$describe the spontaneous nature of the adsorption process. As the temperature increases, $\Delta G°$increase as well, indicating less driving force and hence slower adsorption capacity at higher temperatures[60].

The negative value of$\Delta H°$indicates thatthe adsorption processis exothermic. This magnitudeis related toadsorbateinteractionswith the adsorbentandrearrangement of thesurfaceduring theadsorption process.It is alsoobservedexperimentallyas the fractionof the surface that iscoveredbyadsorbate. Enthalpy change data is useful for distinguishing physisorptionandchemisorption.The typical value for physisorption usually lies below 84 kJ

mol^{-1}, which agrees with the value obtained for MV 2B adsorption onto HNT-Fe$_3$O$_4$; for chemisorption, bond strengths lie between 84 and 420 kJ mol^{-1}. Finally, the results of $\Delta S°$ indicate decreased randomness at the solid/solute interface during the adsorption of MV 2B onto the HNT-Fe$_3$O$_4$ composite [60].This behavior (negative values of $\Delta G°$, $\Delta H°$ and $\Delta S°$; slower adsorption capacity at higher temperatures and physisorption) wasalso observed by others researchers thatemployed magnetic composites for removal of dyes[61-63].

Table 4

Thermodynamics parameters for the adsorption of MV 2B onto HNT-Fe$_3$O$_4$ composite.

Temperature	Thermodynamics			
(K)	$\Delta G°$ (kJ mol^{-1})	$\Delta H°$ (kJ mol^{-1})	$\Delta S°$ (J mol^{-1} K^{-1})	r
283	− 4.09			
293	− 3.75	− 13.23	− 32.32	0.9744
303	− 3.44			

3.6 Reusability of HNT-Fe$_3$O$_4$ composite

It is crucial to investigate the reusability of adsorbents for practical applications to address ecological and economic demands for sustainability[64].Adsorption experiments were performed at a 700 rpm stirring rate anda pH equal to 7.0 with 0.15 g of composite in25mL ofa 90 mg L^{-1} solution of MV2B at25°C for 6 h. After each adsorption experiment, the adsorbent was collected by external magnet force(3000 G) andrecovered by a 1.0 mol L^{-1}solution of NaOH at 250 rpm for 3 h. Then, the HNT-Fe$_3$O$_4$ composite was removed from the alkaline solution and placed in a 0.5% v/v acetic acid solution at the same stirring rate and

contact time. Finally, it was washed several times with distilled water, dried and reused again.The effect of recycling times of HNT-Fe$_3$O$_4$ composite on MV 2B adsorption performance was repeated four times.

Fig. 12 showed that the removal percentage of MV 2B was still near80% after four cycles, indicating that HNT-Fe$_3$O$_4$can be reused. The decrease in *%R*might be due to irreversible adsorption of the adsorbent during the regeneration process[64].
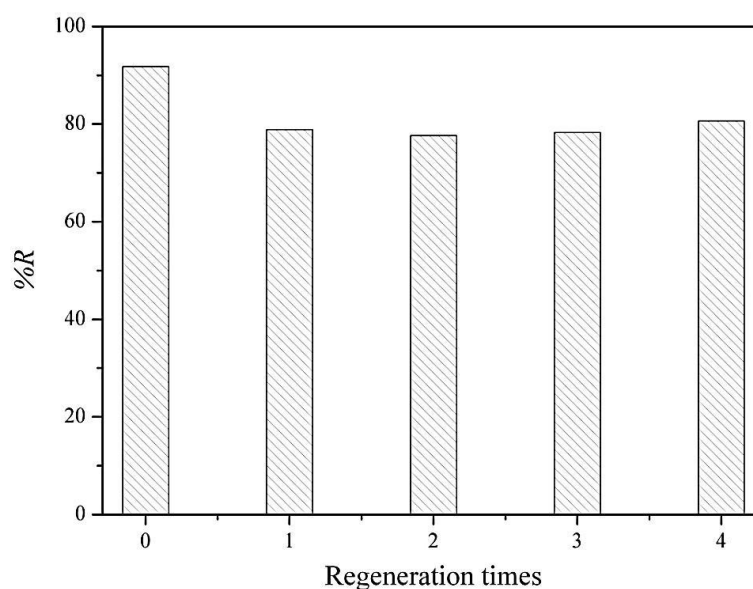

Fig. 12. Reusability cycles of HNT-Fe$_3$O$_4$ composite.

4 Conclusion

In general, the method used to prepare the HNT-Fe$_3$O$_4$ composite was efficient, as shown by the characterization analysis, which verified that the magnetite nanoparticles are anchored onto the surface of the HNT.

The kinetics of the adsorption process wasshown to be better described by a pseudo-second-order model. The experimental results also suggest that both the Langmuir and

Freundlich models were suitable to predict adsorption equilibrium.The experimental data concerning the Langmuir constant (k_L), maximum adsorption capacity (q_m),Freundlich constant (k_F), and $1/n$ were 0.112 mg L^{-1}, 20.04 mg g^{-1}, 5.835 L g^{-1} and 0.2696, respectively. Moreover, the thermodynamic data have shown that the adsorption of MV 2B onto HNT-Fe$_3$O$_4$ composite is a spontaneous and exothermal process by physisorption.

Finally, the employed composite could also be regenerated at least four times using a 1.0 mol L^{-1} solution of NaOH as an eluent and was shown to be a promising adsorbentfor the removal ofMV 2B cationic dye.

References

[1] V.K. Gupta, Suhas, Application of low-cost adsorbents for dye removal − A review, J. Environ. Manage. 90 (2009) 2313-2342.

[2] E. Forgacs, T. Cserháti, G. Oros, Removal of synthetic dyes from wastewaters: a review, Environ. Int. 30 (2004) 953-971.

[3] L. Pereira, M. Alves, Dyes-Environmental Impact and Remediation, in: A. Malik, E. Grohmann (Eds.) Environmental Protection Strategies for Sustainable Development, Springer, New York, 2012, pp. 111-162.

[4]   A. Mittal, V. Gajbe, J. Mittal, Removal and recovery of hazardous triphenylmethane dye, Methyl Violet through adsorption over granulated waste materials, J. Hazard. Mater. 150 (2008) 364-375.

[5]   J. Pal, M. Deb, D. Deshmukh, B. Sen, Microwave-assisted synthesis of platinum nanoparticles and their catalytic degradation of methyl violet in aqueous solution, Appl. Nanosci. 4 (2014) 61-65.

[6]   A.E. Ofomaja, E.E. Ukpebor, S.A. Uzoekwe, Biosorption of Methyl violet onto palm kernel fiber: Diffusion studies and multistage process design to minimize biosorbent mass and contact time, Biomass Bioenergy 35 (2011) 4112-4123.

[7]   M. Esteva, A.M. Ruiz, A.M. Stoka, Trypanosoma cruzi: methoprene is a potent agent to sterilize blood infected with trypomastigotes, Exp. Parasitol. 100 (2002) 248-251.

[8]   S. Laube, Skin infections and ageing, Ageing Res. Rev. 3 (2004) 69-89.

[9]   M. Saji, S. Taguchi, K. Uchiyama, E. Osono, N. Hayama, H. Ohkuni, Efficacy of gentian violet in the eradication of methicillin-resistant Staphylococcus aureus from skin lesions, J. Hosp. Infect. 31 (1995) 225-228.

[10]   M. Wainwright, Dyes for the medical industry, in: M. Clark (Ed.) Handbook of textile and industrial dyeing, Woodhead Publishing Limited, Cambridge, 2011, pp. 204-230.

[11]   P. Li, Y.-J. Su, Y. Wang, B. Liu, L.-M. Sun, Bioadsorption of methyl violet from aqueous solution onto Pu-erh tea powder, J. Hazard. Mater. 179 (2010) 43-48.

[12]   H. Zollinger, Color chemistry: syntheses, properties and applications of organic dyes and pigments, 2 ed., VCH, Weinheim, 1991.

[13]   R.W. Sabnis, Handbook of Biological Dyes and Stains, John Wiley & Sons, New Jersey, 2010.

[14]   S. Chakraborty, S. Chowdhury, P. Das Saha, Adsorption of Crystal Violet from aqueous solution onto NaOH-modified rice husk, Carbohydr. Polym. 86 (2011) 1533-1541.

[15] F. Chen, P. Fang, Y. Gao, Z. Liu, Y. Liu, Y. Dai, Effective removal of high-chroma crystal violet over TiO_2-based nanosheet by adsorption–photocatalytic degradation, Chem. Eng. J. 204–206 (2012) 107-113.

[16] Z. Chen, T. Wang, X. Jin, Z. Chen, M. Megharaj, R. Naidu, Multifunctional kaolinite-supported nanoscale zero-valent iron used for the adsorption and degradation of crystal violet in aqueous solution, J. Colloid Interf. Sci. 398 (2013) 59-66.

[17] M.A. Gabal, E.A. Al-Harthy, Y.M. Al Angari, M. Abdel Salam, MWCNTs decorated with $Mn_{0.8}Zn_{0.2}Fe_2O_4$ nanoparticles for removal of crystal-violet dye from aqueous solutions, Chem. Eng. J. 255 (2014) 156-164.

[18] A. Pal, S. Pan, S. Saha, Synergistically improved adsorption of anionic surfactant and crystal violet on chitosan hydrogel beads, Chem. Eng. J. 217 (2013) 426-434.

[19] K.P. Singh, S. Gupta, A.K. Singh, S. Sinha, Optimizing adsorption of crystal violet dye from water by magnetic nanocomposite using response surface modeling approach, J. Hazard. Mater. 186 (2011) 1462-1473.

[20] Y.S. Al-Degs, M.I. El-Barghouthi, A.H. El-Sheikh, G.M. Walker, Effect of solution pH, ionic strength, and temperature on adsorption behavior of reactive dyes on activated carbon, Dyes Pigm. 77 (2008) 16-23.

[21] P.C. Vandevivere, R. Bianchi, W. Verstraete, Treatment and reuse of wastewater from the textile wet-processing industry: Review of emerging technologies, J. Chem. Technol. Biotechnol. 72 (1998) 289-302.

[22] M.T. Yagub, T.K. Sen, S. Afroze, H.M. Ang, Dye and its removal from aqueous solution by adsorption: A review, Adv. Colloid Interface Sci. 209 (2014) 172-184.

[23] J. Bujdák, Effect of the layer charge of clay minerals on optical properties of organic dyes. A review, Appl. Clay Sci. 34 (2006) 58-73.

[24] F. Zhao, W.Z. Tang, D. Zhao, Y. Meng, D. Yin, M. Sillanpää, Adsorption kinetics, isotherms and mechanisms of Cd(II), Pb(II), Co(II) and Ni(II) by a modified magnetic polyacrylamide microcomposite adsorbent, J. Water Process Eng. 4 (2014) 47-57.

[25] L. Ai, Y. Zhou, J. Jiang, Removal of methylene blue from aqueous solution by montmorillonite/$CoFe_2O_4$ composite with magnetic separation performance, Desalination 266 (2011) 72-77.

[26] X.-F. Sun, B. Liu, Z. Jing, H. Wang, Preparation and adsorption property of xylan/poly(acrylic acid) magnetic nanocomposite hydrogel adsorbent, Carbohydr. Polym. 118 (2015) 16-23.

[27] V.K. Gupta, S. Agarwal, T.A. Saleh, Chromium removal by combining the magnetic properties of iron oxide with adsorption properties of carbon nanotubes, Water Res. 45 (2011) 2207-2212.

[28] V. Rocher, J.-M. Siaugue, V. Cabuil, A. Bee, Removal of organic dyes by magnetic alginate beads, Water Res. 42 (2008) 1290-1298.

[29] R. Sivashankar, A.B. Sathya, K. Vasantharaj, V. Sivasubramanian, Magnetic composite an environmental super adsorbent for dye sequestration – A review, Environ. Nanotechnol. Monitor. Manage. 1–2 (2014) 36-49.

[30] Y.-P. Chang, C.-L. Ren, J.-C. Qu, X.-G. Chen, Preparation and characterization of Fe_3O_4/graphene nanocomposite and investigation of its adsorption performance for aniline and p-chloroaniline, Appl. Surf. Sci 261 (2012) 504-509.

[31] J. Duan, R. Liu, T. Chen, B. Zhang, J. Liu, Halloysite nanotube-Fe_3O_4 composite for removal of methyl violet from aqueous solutions, Desalination 293 (2012) 46-52.

[32] J. Pan, H. Yao, L. Xu, H. Ou, P. Huo, X. Li, Y. Yan, Selective Recognition of 2,4,6-Trichlorophenol by Molecularly Imprinted Polymers Based on Magnetic Halloysite Nanotubes Composites, J. Phys. Chem. C 115 (2011) 5440-5449.

[33] Y. Xie, D. Qian, D. Wu, X. Ma, Magnetic halloysite nanotubes/iron oxide composites for the adsorption of dyes, Chem. Eng. J. 168 (2011) 959-963.

[34] S. Yang, P. Zong, J. Hu, G. Sheng, Q. Wang, X. Wang, Fabrication of β-cyclodextrin conjugated magnetic HNT/iron oxide composite for high-efficient decontamination of U(VI), Chem. Eng. J. 214 (2013) 376-385.

[35] Y. Zhang, H. Yang, Halloysite nanotubes coated with magnetic nanoparticles, Appl. Clay Sci. 56 (2012) 97-102.

[36] Z. Zhang, J. Kong, Novel magnetic Fe_3O_4@C nanoparticles as adsorbents for removal of organic dyes from aqueous solution, J. Hazard. Mater. 193 (2011) 325-329.

[37] I.D. Mall, V.C. Srivastava, G.V.A. Kumar, I.M. Mishra, Characterization and utilization of mesoporous fertilizer plant waste carbon for adsorptive removal of dyes from aqueous solution, Colloids Surf. Physicochem. Eng. Aspects 278 (2006) 175-187.

[38] Y. Lvov, E. Abdullayev, Functional polymer–clay nanotube composites with sustained release of chemical agents, Prog. Polym. Sci. 38 (2013) 1690-1719.

[39] E. Joussein, S. Petit, J. Churchman, B. Theng, D. Righi, B. Delvaux, Halloysite clay minerals — a review, Clay Miner. 40 (2005) 383-426.

[40] C. Salazar-Camacho, M. Villalobos, M.d.l.L. Rivas-Sánchez, J. Arenas-Alatorre, J. Alcaraz-Cienfuegos, M.E. Gutiérrez-Ruiz, Characterization and surface reactivity of natural and synthetic magnetites, Chem. Geol. 347 (2013) 233-245.

[41] B.v. Raij, Determinação do ponto de carga zero em solos, Bragantia 32 (1973) 337-347.

[42] M. Suzuki, Adsorption engineering, Kodansha, Tokyo, 1990.

[43] N.F. Cardoso, R.B. Pinto, E.C. Lima, T. Calvete, C.V. Amavisca, B. Royer, M.L. Cunha, T.H.M. Fernandes, I.S. Pinto, Removal of remazol black B textile dye from aqueous solution by adsorption, Desalination 269 (2011) 92-103.

[44] T. Calvete, E.C. Lima, N.F. Cardoso, S.L.P. Dias, F.A. Pavan, Application of carbon adsorbents prepared from the Brazilian pine-fruit-shell for the removal of Procion Red MX 3B from aqueous solution—Kinetic, equilibrium, and thermodynamic studies, Chem. Eng. J. 155 (2009) 627-636.

[45] E.F.J. Duynstee, E. Grunwald, Organic Reactions Occurring in or on Micelles. II. Kinetic and Thermodynamic Analysis of the Alkaline Fading of Triphenylmethane Dyes in the Presence of Detergent Salts1, J. Am. Chem. Soc. 81 (1959) 4542-4548.

[46] R. Liu, B. Zhang, D. Mei, H. Zhang, J. Liu, Adsorption of methyl violet from aqueous solution by halloysite nanotubes, Desalination 268 (2011) 111-116.

[47] K.A. Guimarães Gusmão, L.V. Alves Gurgel, T.M. Sacramento Melo, L.F. Gil, Application of succinylated sugarcane bagasse as adsorbent to remove methylene blue and gentian violet from aqueous solutions − Kinetic and equilibrium studies, Dyes Pigm. 92 (2012) 967-974.

[48] B.H. Hameed, Equilibrium and kinetic studies of methyl violet sorption by agricultural waste, J. Hazard. Mater. 154 (2008) 204-212.

[49] W. Plazinski, W. Rudzinski, A. Plazinska, Theoretical models of sorption kinetics including a surface reaction mechanism: A review, Adv. Colloid Interface Sci. 152 (2009) 2-13.

[50] Y.S. Ho, G. McKay, Pseudo-second order model for sorption processes, Process Biochem. 34 (1999) 451-465.

[51] E.C. Lima, B. Royer, J.C.P. Vaghetti, J.L. Brasil, N.M. Simon, A.A. dos Santos Jr, F.A. Pavan, S.L.P. Dias, E.V. Benvenutti, E.A.d. Silva, Adsorption of Cu(II) on *Araucaria angustifolia* wastes: Determination of the optimal conditions by statistic design of experiments, J. Hazard. Mater. 140 (2007) 211-220.

[52] K.Y. Foo, B.H. Hameed, Insights into the modeling of adsorption isotherm systems, Chem. Eng. J. 156 (2010) 2-10.

[53] S. Rangabhashiyam, N. Anu, M.S. Giri Nandagopal, N. Selvaraju, Relevance of isotherm models in biosorption of pollutants by agricultural byproducts, J. Environ. Chem. Eng. 2 (2014) 398-414.

[54] C. Namasivayam, M.V. Sureshkumar, Modelling Thiocyanate Adsorption onto Surfactant-Modified Coir Pith, an Agricultural Solid 'Waste', Process Saf. Environ. 85 (2007) 521-525.

[55] M.H. Kalavathy, L.R. Miranda, Comparison of copper adsorption from aqueous solution using modified and unmodified Hevea brasiliensis saw dust, Desalination 255 (2010) 165-174.

[56] J.-S. Wu, C.-H. Liu, K.H. Chu, S.-Y. Suen, Removal of cationic dye methyl violet 2B from water by cation exchange membranes, J. Membr. Sci. 309 (2008) 239-245.

[57] G. Annadurai, R.-S. Juang, D.-J. Lee, Use of cellulose-based wastes for adsorption of dyes from aqueous solutions, J. Hazard. Mater. 92 (2002) 263-274.

[58] A.E. Ofomaja, Kinetic study and sorption mechanism of methylene blue and methyl violet onto mansonia (*Mansonia altissima*) wood sawdust, Chem. Eng. J. 143 (2008) 85-95.

[59] J. Saikia, Y. Sikdar, B. Saha, G. Das, Malachite nanoparticle: A potent surface for the adsorption of xanthene dyes, J. Environ. Chem. Eng. 1 (2013) 1166-1173.

[60] K. Fujiwara, A. Ramesh, T. Maki, H. Hasegawa, K. Ueda, Adsorption of platinum (IV), palladium (II) and gold (III) from aqueous solutions onto l-lysine modified crosslinked chitosan resin, J. Hazard. Mater. 146 (2007) 39-50.

[61] W. Konicki, D. Sibera, E. Mijowska, Z. Lendzion-Bieluń, U. Narkiewicz, Equilibrium and kinetic studies on acid dye Acid Red 88 adsorption by magnetic $ZnFe_2O_4$ spinel ferrite nanoparticles, J. ColloidInterf. Sci. 398 (2013) 152-160.

[62] G.R. Mahdavinia, A. Massoudi, A. Baghban, E. Shokri, Study of adsorption of cationic dye on magnetic *kappa*-carrageenan/PVA nanocomposite hydrogels, J. Environ. Chem. Eng. 2 (2014) 1578-1587.

[63] S. Zeng, S. Duan, R. Tang, L. Li, C. Liu, D. Sun, Magnetically separable $Ni_{0.6}Fe_{2.4}O_4$ nanoparticles as an effective adsorbent for dye removal: Synthesis and study on the kinetic and thermodynamic behaviors for dye adsorption, Chem. Eng. J. 258 (2014) 218-228.

[64] C. Cao, L. Xiao, C. Chen, X. Shi, Q. Cao, L. Gao, In situ preparation of magnetic Fe_3O_4/chitosan nanoparticles via a novel reduction–precipitation method and their application in adsorption of reactive azo dye, Powder Technol. 260 (2014) 90-97.